arXiv:1704.04042v1 [cond-mat.supr-con] 13 Apr 2017

Higgs-mode radiance and charge-density-wave order in 2H-$NbSe_2$

Romain Grasset,[1] Tommaso Cea,[2,3] Yann Gallais,[1] Maximilien Cazayous,[1]
Alain Sacuto,[1] Laurent Cario,[4] Lara Benfatto,[3,*] and Marie-Aude Méasson[1,†]

[1] *Université Paris Diderot, Sorbonne Paris Cité, CNRS Laboratoire Matériaux et Phénomènes Quantiques, UMR 7162 75013, Paris, France*
[2] *Graphene Labs, Fondazione Istituto Italiano di Tecnologia, Via Morego, 16163 Genova, Italy*
[3] *ISC-CNR and Department of Physics, Sapienza University of Rome, P.le A. Moro 5, 00185 Rome, Italy*
[4] *Institut des Matériaux Jean Rouxel (IMN), Université de Nantes - CNRS, 2 rue de la Houssiniére, BP 32229, 44322 Nantes Cedex 03, France.*

(Dated: April 14, 2017)

Despite being usually considered two competing phenomena, charge-density-wave and superconductivity coexist in few systems, the most emblematic one being the transition metal dichalcogenide 2H-$NbSe_2$. This unusual condition is responsible for specific Raman signatures across the two phase transitions in this compound. While the appearance of a soft phonon mode is a well-established fingerprint of the charge-density-wave order, the nature of the sharp sub-gap mode emerging below the superconducting temperature is still under debate. In this work we use the external pressure as a knob to unveil the delicate interplay between the two orders, and consequently the nature of the superconducting mode. Thanks to an advanced extreme-conditions Raman technique we are able to follow the pressure evolution and the simultaneous collapse of the two intertwined charge density wave and superconducting modes. The comparison with microscopic calculations in a model system supports the Higgs-type nature of the superconducting mode and suggests that charge-density-wave and superconductivity in 2H-$NbSe_2$ involve mutual electronic degrees of freedom. These findings fill knowledge gap on the electronic mechanisms at play in transition metal dichalcogenides, a crucial step to fully exploit their properties in few-layers systems optimized for devices applications.

PACS numbers: 74.70.Ad,71.45.Lr ,74.20.-z,74.25.nd,74.62.Fj

I. INTRODUCTION

The symmetry breaking across an electronic phase transition always occurs along with the emergence of new collective excitations. The charge-density-wave (CDW) electronic instability is accompanied by the softening of a phonon coupled to the electronic density at $\mathbf{Q}_{CDW}$ and dressed by the amplitude fluctuations of the CDW order parameters which develops below T_{CDW}[1, 2]. This new mode, also called amplitudon, is Raman active[3, 4] and has been detected in several CDW dichalcogenides, including 2H-$NbSe_2$[5–7].

In the superconducting (SC) state, two additional collective excitations of the superconducting order parameter are expected: a massless Nambu-Goldstone phase mode, which is pushed to the plasmon frequency in a charged superconductor, and a massive amplitude mode, also named Higgs mode for the analogy with the Higgs boson in high-energy physics[8]. In principle, the Higgs mode remains "dark" to spectroscopy probes, since it weakly couples to the electromagnetic field[9] and is overdamped[4, 10–13]. Indeed its energy coincides with the threshold $2\Delta_{SC}$ of the quasiparticle continuum, Δ_{SC} being the superconducting gap[4, 10–12, 14]. Even though some recent reports investigated the possibility to detect it via optical spectroscopy in rather unconventional situations[15] or intense THz field[16, 17], its presence and observability are still under strong debate[9, 13, 18–20].

On the other hand, when superconductivity coexists with a CDW order the Higgs mode has the unique opportunity to become visible via its coupling to the soft CDW phonon mode. 2H-$NbSe_2$ is one of the few systems where the two orders coexist, with a CDW and superconducting instabilities at $T_{CDW} = 33$ and $T_c = 7$ K, respectively. This mechanism has been proposed long ago[12, 21] to explain the dramatic changes of the Raman spectrum of 2H-$NbSe_2$ below T_c, where a sharp peak develops below $2\Delta_{SC}$ by stealing spectral weight from the soft phonon peak [6, 22]. Nonetheless, other mechanisms could give rise to sharp superconducting resonances, as observed in other multiband superconductors[23, 24], making the assignment of the superconducting peak to the Higgs mode problematic.

Tuning the delicate interplay between the CDW and superconductivity is achievable by application of high pressure or by lowering the dimensionality of the system. Pressure experiments in 2H-$NbSe_2$ showed that above a critical pressure of 4 GPa the CDW order disappears while superconductivity remains almost unaffected[25–28] (Fig. 1a). This behavior is in striking contrast to what is found by reducing the sample dimensionality[7, 29, 30]. All these observations triggered intense theoretical efforts[31–35] to explain the origin of the CDW

* author to whom correspondence should be addressed: lara.benfatto@roma1.infn.it
† author to whom correspondence should be addressed: marie-aude.measson@neel.cnrs.fr; now at : Institut Néel, CNRS and Université Grenoble Alpes, F-38042 Grenoble, France

and superconducting transition in bulk and few-layers 2H-$NbSe_2$, by accounting for the different role of the electron-phonon coupling and Fermi-surface nesting. So far, pressure effects have been addressed via signatures of the lattice and its dynamics [27, 28]. Raman probe under pressure has the advantage to assess directly the evolution of the *electronic* degrees of freedom with the pressure-driven CDW softening, without the additional complication of the interaction with the substrate, relevant in devices based on few-layers 2H-$NbSe_2$.

Here we use an advanced low-temperature and high-pressure technique to probe the Raman signatures of the CDW and superconducting excitations across the phase diagram of 2H-$NbSe_2$. Besides, we compute the evolution of the Raman response within a microscopic model for the coexisting CDW and superconducting order. Our findings unambiguously assign the superconducting peak to the Higgs fluctuations, made Raman visible via the charge-density-wave soft phonon. This result not only provides a perspective for the microscopic mechanisms at play in the coexisting states of 2H-$NbSe_2$, but it also shows that the Higgs-mode radiance is a direct fingerprint of charge ordering.

II. EXPERIMENTAL DETAILS

Single crystals of 2H-$NbSe_2$ were synthesized at 750°C using the iodine-vapour transport method as described elsewhere[36]. The crystallographic quality of several crystals was checked by X-ray diffraction. All crystals revealed a hexagonal cell with parameters a=b=3.44Å and c=12.54Å in agreement with the 2H polytype.

We have adapted an original optical experimental setup (Fig. 1b) to probe low energy Raman excitations under extreme conditions of pressure and low temperature. This report constitutes the first experiment of this type, successfully reaching low energy probe down to 7 cm^{-1} (0.85 meV) down to $\sim$ 3 K and up to 5 GPa. We have thus been able to track simultaneously the superconducting and the CDW modes under a broad range of hydrostatic pressure. Raman scattering measurements have been performed on freshly cleaved 2H-$NbSe_2$ crystal with an incident angle of $\sim 30°$ with respect to the sample surface normal and in a membrane diamond anvils cell designed for a large numerical aperture together with a low Raman signal from the environment of the sample as described in [37]. The pressure cell was cooled down in a closed-cycle ^{4}He cryostat with a base temperature of 3 K. As sketched in Fig. 1a, a OFHC Cooper braid between the metallic gasket and the cold finger is used as a cryogenic leakage. This, together with a low laser incident power (typically 0.1 mW), control of the size of the incident laser spot (about 20 μm diameter) allowed to reach low temperature, estimated between 3 and 3.5 K, low-enough to measure a Raman signature of the superconducting state of 2H-$NbSe_2$ (T_c = 7.2 K).

We have used a triple-grating spectrometer Jobin Yvon T64000 equipped with a liquid-nitrogen-cooled CCD detector and the 532 nm excitation line from a solid-state laser. The polarization of the incoming and outgoing light are in the (ab) plane of the sample. In this configuration, in parallel and crossed polarizations we select the A_{1g}+E_{2g} and the E_{2g} symmetries, respectively. Birefringence of the diamonds under pressure mixes the effective polarization of lights. Extraction of pure E_{2g} and A_{1g} symmetries was done by scaling the E_{2g} phonon mode at about 250 cm^{-1}. The fluorescence of ruby has been used as a pressure gauge. The pressure transmitting medium is ^{4}He. It does not show any particular Raman features at low energy (down to 7 cm^{-1}), down to 3 K and up to 10 GPa.

III. COLLAPSE OF THE COLLECTIVE MODES

A typical spectrum of 2H-$NbSe_2$ under high pressure (2 GPa) and at low temperature in the coexisting region of CDW and SC states is displayed in Fig 1(c) in a large Raman shift range. In the mixed A_{1g}+E_{2g} symmetry, beyond the single phonons E^2_{2g}, E_{1g} and E^1_{2g} (at 26, 238 and 252 cm^{-1}, respectively), a second-order phonon peak ($\sim$ 130 cm^{-1}) and a CDW-phonon ($\sim$ 200 cm^{-1}, marked with $\star$) are observed. The last one is a signature of the CDW ordering, most probably a phonon mode folded to the zone center due to the CDW ordering. It remains a hard mode up to T_{CDW} while the low energy collective modes at $\sim$ 15 cm^{-1} and $\sim$ 40 cm^{-1} soften upon approaching the ordering temperatures T_{SC} and T_{CDW}, respectively. Both these SC and CDW collective modes are visible in the fully symmetrical A_{1g} and the in-plane symmetry breaking E_{2g} channels. The CDW soft mode has been assigned to the instability phonon dressed by amplitude fluctuations of the CDW, the so called amplitudon[5]. As already discussed [6], a partial spectral weight transfer from the CDW mode to the SC mode exists with decreasing temperature. While the Higgs mode rises, the CDW soft mode looses spectral weight, as observed in the two different symmetries E_{2g} and A_{1g} (see Appendix B).

As presented in Fig. 2(a), by applying high pressure above 4 GPa (Fig. 1(c)) a pure superconducting state is reached and the CDW mode disappears while a superconducting signature persists in the E_{2g} symmetry. Nevertheless, its intensity is much reduced by a factor of ~ 8 and its energy hardens. As shown in the inset of Fig. 2(a), the superconducting Raman response of the superconducting compound 2H-NbS_2 which lacks the CDW state at ambient pressure [6] matches perfectly that of 2H-$NbSe_2$ above the critical pressure, P_c, in the pure superconducting state as long as the Raman shift is scaled by $2\Delta_{SC}$ (Δ_{SC} is calculated from the value of the superconducting gap measured by STM [39] and its pressure dependence is scaled as T_c(P)[26]). Both superconducting thresholds are positioned at $2\Delta_{SC}$ as expected for

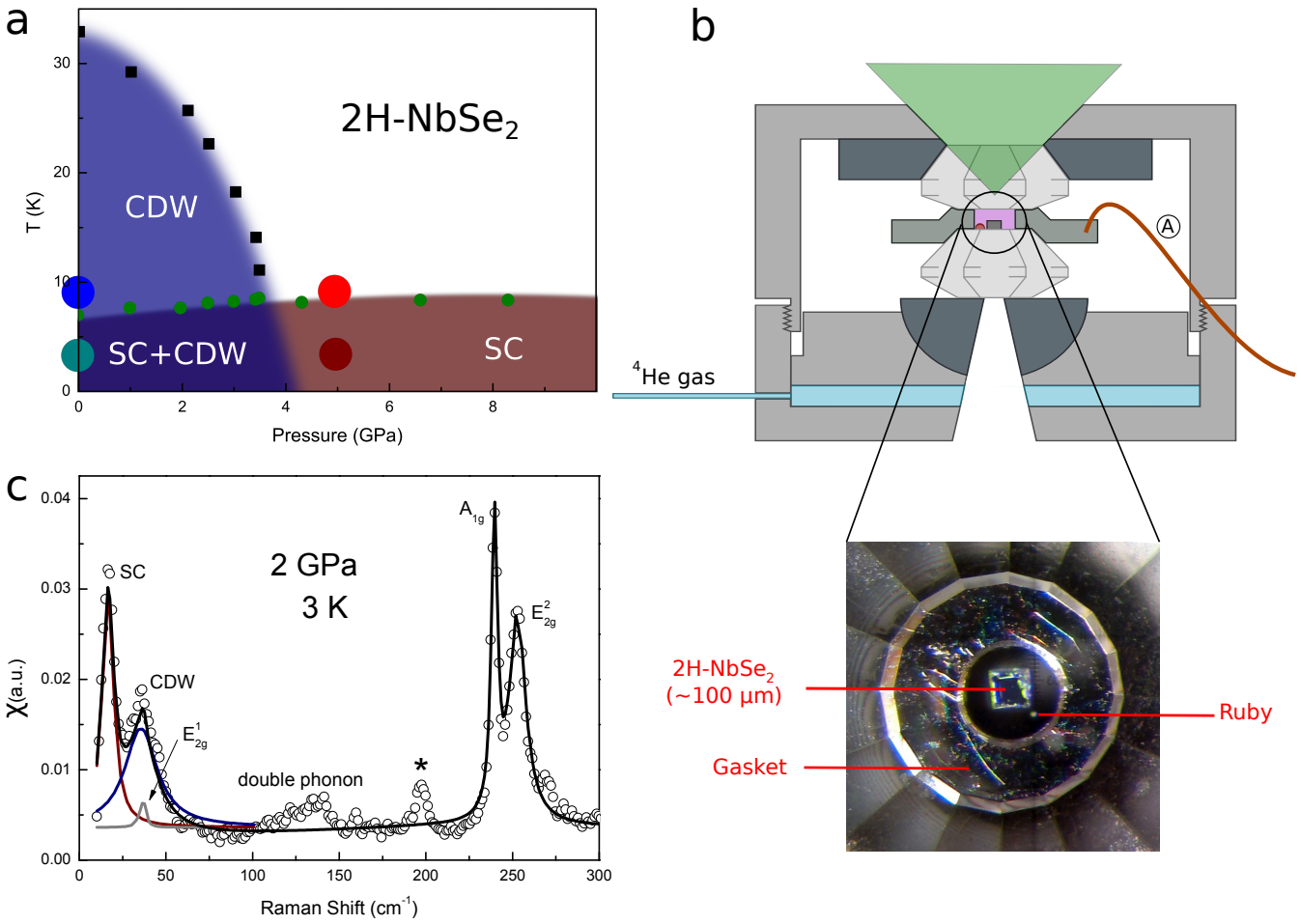

FIG. 1. Raman scattering under hydrostatic pressure and at low temperature of 2H-$NbSe_2$. (a) (P,T) Phase diagram of 2H-$NbSe_2$ drawn from resistivity measurements[26, 38]. The incommensurate CDW collapses at a critical pressure of $\sim$ 4 GPa, a pure SC state persists up to at least 10 GPa. Large colored circles mark the (P,T) positions of the experimental spectra reported in Fig.2(a). (b) Membrane Diamond anvil cell designed for a large numerical aperture collection, low Raman signal from the environment and access to low temperature ($\sim$ 3 K). The 350 μm diameter pressure chamber containing the freshly cleaved 2H-$NbSe_2$ sample and rubies as pressure gauge is depicted below. (A) Thermal link between the metallic gasket and the cold finger of the cryostat made of high conductivity Cooper wires. (c) Raman spectra of 2H-$NbSe_2$ in the A_{1g}+E_{2g} symmetry at 2 GPa and 3 K in the coexisting region of charge-density-wave and superconducting orders. the $\star$ designs a CDW-phonon mode. Consistently with the theory, the two collective excitations at 15 cm^{-1} and 40 cm^{-1} are assigned to the Higgs superconducting mode and the charge-density-wave amplitudon mode.

a simple Cooper-pair breaking peak. Consistently with this assignment, there is no signature of the pure superconducting state, reached above the critical pressure, in the A_{1g} symmetry in 2H-$NbSe_2$, due to Coulomb screening effect [40–42](see Appendix A). At a pressure below P_c, the energies of the superconducting modes are always below $2\Delta_{SC}$ as shown in Fig. 2c. Furthermore, the A_{1g} mode softens by 30 % and the energy of the E_{2g} mode stays constant whereas the critical temperature T_c rises with pressure. The absence of scaling between the superconducting peak energy and T_{SC} in the SC+CDW coexisting phase indicates that both SC modes are not simple Cooper pairs breaking peaks. Moreover the disappearance of the sharp superconducting mode below $2\Delta_{SC}$ in the pure superconducting phase demonstrates unambiguously its intimate link with the coexisting charge-density-wave order. These findings, consistently with the theory discussed below, support the Higgs type assignment of the superconducting modes.

IV. COMPARISON WITH A MICROSCOPIC MODEL

In 2H-$NbSe_2$ the phonon coupled to the CDW belongs to an acoustic branch, so the single-phonon mode is not visible as a finite-energy peak in $\mathbf{q}\sim 0$ Raman spectroscopy above T_{CDW}. Below T_{CDW} the intermediate

electron-hole excitations which couple directly to light allow to make the phonon mode at $\mathbf{Q}_{CDW}$ Raman visible at $\mathbf{q} = 0$. This gives rise to the soft phonon modes at $\sim$ 40cm^{-1}. In a general approach, the Raman response below T_{CDW} can be schematically written as

$$\chi"(\omega) = Z_{eff}(T, \Delta_{CDW}) \frac{\Gamma_{ph}}{(\omega^2 - \Omega_0^2(T))^2 + \Gamma_{ph}^2} \quad (1)$$

where the soft mode frequency $\Omega_0(T)$ and damping Γ_{ph} are both determined by the CDW amplitude fluctuations and the prefactor $Z_{eff} \sim \Delta_{CDW}^2$ grows proportionally to the CDW order parameter[4]. The frequency $\Omega_0(T)$ also scales approximately with the CDW gap, so it goes to zero at T_{CDW}, even though the Raman peak disappears already at $T \simeq 0.9T_{CDW}$ due to the strong suppression of Z_{eff}. Upon entering the superconducting state, the phonon spectrum is modified by the coupling to the superconducting Higgs fluctuations, as originally proposed by Littlewood and Varma[12]. This gives rise to the additional, sharp resonance below $2\Delta_{SC}$, at $\sim$ 15 cm^{-1}. In that sense, the superconducting signature is not expected to be the pure Higgs mode. Rather we observe its manifestation on the CDW amplitudon, which is split thanks to the interaction with the Higgs fluctuations.

This scenario can be made quantitative via the explicit calculation of the Raman response within a microscopic model system for the coexisting state. This calculation accounts for two crucial ingredients: (i) the coupling between the soft phonon and the Higgs fluctuations, which originates microscopically[4, 43] from the intertwined amplitude fluctuations of the two CDW and SC order parameters, and (ii) the evaluation of the intermediate electron-hole processes which make the CDW phonon Raman visible. The item (i) implies also that the CDW and SC order parameters should overlap at least in part of the Fermi surface, so that their amplitude fluctuations talk to each other via a modification of the same electronic density-of-state. As it has already been shown in Ref. [4], this calculation is able to reproduce successfully the main feature of the experiments at ambient pressure. Here, following the same approach, we model the pressure effects by a continuous suppression of the coupling g_{CDW} in the CDW channel with respect to the initial value g^0_{CDW} (see Appendix D). By computing self-consistently the values of the order parameters we find that above a critical value of $\alpha = (g_{CDW} - g^0_{CDW})/g^0_{CDW}$ the CDW gap at $T = 0$ vanishes, leaving only the SC instability. The Raman intensities are then computed in the various phases (pure SC, CDW+SC, CDW such as measured) (Fig. 2(b)). The spectra have the same absolute units, so the scaling of the intensities is respected. The theoretical Raman response is consistent with our measurements: the Higgs mode manifests as a secondary peak of the CDW soft phonon, which is the mode Raman visible. Thus it appears as a sub-gap intense peak only when it coexists with a CDW state. When the CDW disappears the Raman response in the pure superconducting state is a broad and weak mode at $2\Delta_{SC}$. Besides, the hardening and damping of the phonon mode upon entering the SC state is a direct consequence of its coupling to the collective electronic excitations, whose density of states gets redistributed from below to above $2\Delta_{SC}$ in the superconducting state.

V. TUNING THE INTERPLAY BETWEEN CDW AND SC WITH PRESSURE

To further unveil the interplay between CDW and SC in 2H-$NbSe_2$ we have finely tuned the pressure in the coexisting CDW+SC state, both experimentally and theoretically. Figure 3(a) and 3(b) reports the experimental results below and above T_{SC}, respectively, from ambient pressure up to 3.67 GPa. The intensities are normalized on the high energy E_{2g} phonon mode. The CDW mode gradually softens (also see Appendix C), enlarges and looses intensity with increasing pressure while the SC mode looses intensity but remains sizable even when the CDW mode is almost invisible (for instance at 3.54 GPa and 3.67 GPa). At all pressures up to the critical pressure, the shift to higher energy of the CDW mode and its enlargement upon entering the SC state as well as the transfer of spectral weight from the CDW modes to the SC modes are observed (see Appendix B). The pressure trend of the CDW and SC modes is well reproduced by our calculations as shown in Fig. 3(c) and 3(d). As we change the CDW coupling the CDW gap Δ_{CDW} is suppressed, while Δ_{SC} stays approximately constant (see inset). The energy of the amplitudon then softens since the CDW amplitude fluctuations are peaked at $2\Delta_{CDW}$. Simultaneously the Raman intensity Z_{eff} is rapidly suppressed, making the Raman signature of the CDW peak above T_{SC} barely visible. Therefore, as the system is cooled below T_{SC} the radiance of the sharp Higgs signature guarantees that a residual CDW order is present.

The evolution of the Higgs-like peak position with pressure is quite striking. In the A_{1g} channel it softens with increasing pressure, in agreement with our calculations (Fig. 3(c)), while in the E_{2g} symmetry it remains roughly constant in energy until the critical pressure (Fig. 2c). In our simplified model the CDW instability occurs at a single $\mathbf{Q}_{CDW}$ vector equivalent to half of the reciprocal-lattice wavevector. In this situation, the CDW phonon is only visible in the fully symmetrical A_{1g} channel. On the other hand, in 2H-$NbSe_2$ the CDW instability can occur at three equivalent $\mathbf{Q}^i_{CDW}$ wavevectors connected by a $2\pi/3$ rotation. This guarantees that the soft phonon mode has a finite projection in both A_{1g} and E_{2g} symmetries[3]. When the SC state forms the Higgs fluctuations renormalize the frequencies of the phonon modes corresponding to lattice displacements at the three $\mathbf{Q}^i_{CDW}$ wavevector. If the electron-phonon coupling has a non-trivial momentum dependence, as it has been emphasized recently[32, 34], one cannot exclude a splitting of the Higgs signatures, which reflects in a different trend of the subgap peak observed in the A_{1g} and

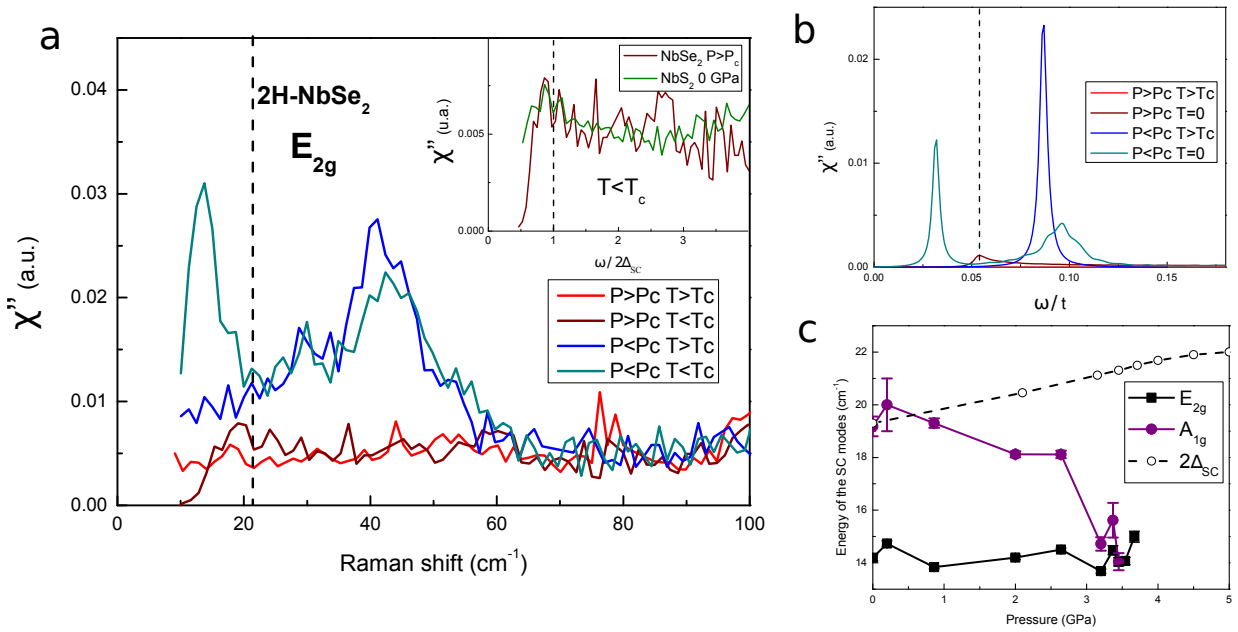

FIG. 2. Collapse of the Higgs mode in the pure superconducting state of 2H-$NbSe_2$, measurements and theoretical predictions. (a) Raman spectra in the E_{2g} symmetry measured in various (P,T) positions as identified Fig. 1(c) : in the coexisting SC+CDW (green) and pure CDW (blue) states at ambient pressure and in the pure SC (brown) and paramagnetic (red) state at high pressure. Both the CDW amplitudon and the SC Higgs modes disappear at high pressure. A small Cooper pairs breaking peak remains at $2\Delta_{SC}$, as marked by the vertical dot line. Inset: Raman spectra in the pure SC state of 2H-$NbSe_2$ under pressure and non-CDW NbS_2 (0 GPa) versus the Raman shift normalized to $2\Delta_{SC}$. (b) Theoretical Raman responses calculated in a microscopic model (see text and Appendix D) in the four phases (SC+CDW, CDW, SC,PM) for comparison with the experimental spectra in (a) t is the hopping term. The parameters are: Δ_{SC}/t=0.025, g_{CDW}/t=0.14 and 0.12 in the SC+CDW and SC phases, respectively. The spectra are well-reproduced in all phases. (c) Pressure dependence of the energy of the SC mode in the two different channels A_{1g} and E_{2g} and of $2\Delta_{SC}$ extracted from STM measurements at $P = 0$ GPa and scaled with T_{SC} versus P[26, 39]. From 0 to 4GPa, the A_{1g} mode softens by 30% whereas the E_{2g} one is constant, showing strong symmetry-dependent behavior.

E_{2g} channel under pressure. A full understanding of this issue requires a calculation within a microscopic model for 2H-$NbSe_2$, that is beyond the scope of the present paper.

VI. DISCUSSION

The comparison between the theoretical calculations and the experiments reported in Fig. 2 and Fig. 3 strongly supports the assignment of the SC peak to a signature of the Higgs mode carried out by the phonon peak. In particular, the sudden disappearance of the SC signature as $\Delta_{CDW} = 0$ agrees with the general prediction of Eq. (1) that its Raman visibility is only guaranteed by the presence of a soft, Raman-active CDW phonon, allowing for $Z_{eff} \neq 0$. Indeed, other possible interpretations based on the multiband structure of 2H-$NbSe_2$, like a Leggett mode or a Bardasis-Schrieffer mode, cannot be easily reconciled with this behavior, since they are intimately related to the properties of the SC state, which barely changes as a function of pressure. For example the Leggett mode, due to the relative fluctuations of the SC phases in two bands, becomes Raman visible thanks to the hole/electron character of the various bands[23, 42], which are not expected to change with pressure. The Bardasis-Schrieffer mode can manifest as a sharp mode below $2\Delta_{SC}$[44]. It originates from subleading pairing fluctuations, so it should be observed in a Raman channel orthogonal to the one where the driving SC instability occurs[44]. Thus, since 2H-$NbSe_2$ is a s-wave superconductor the Bardasis-Schrieffer mode should *not* be visible in the A_{1g} channel[44], in contrast with our experimental results.

As we mentioned above, we computed the Raman intensity in the coexisting CDW and SC state with a model Hamiltonian (see Appendix D) that is not intended to reproduce realistically 2H-$NbSe_2$. This implies for example that in our approach the CDW originates from a Fermi-surface nesting instability, while in 2H-$NbSe_2$ it has been clearly shown that the electronic susceptibility gets strongly enhanced at the ordering wavevector $\mathbf{Q}_{CDW}$ only when the momentum dependence of the electron-phonon coupling is taken into account[32, 34]. However, once this effect is included the description of the CDW state does not differ conceptually from a standard

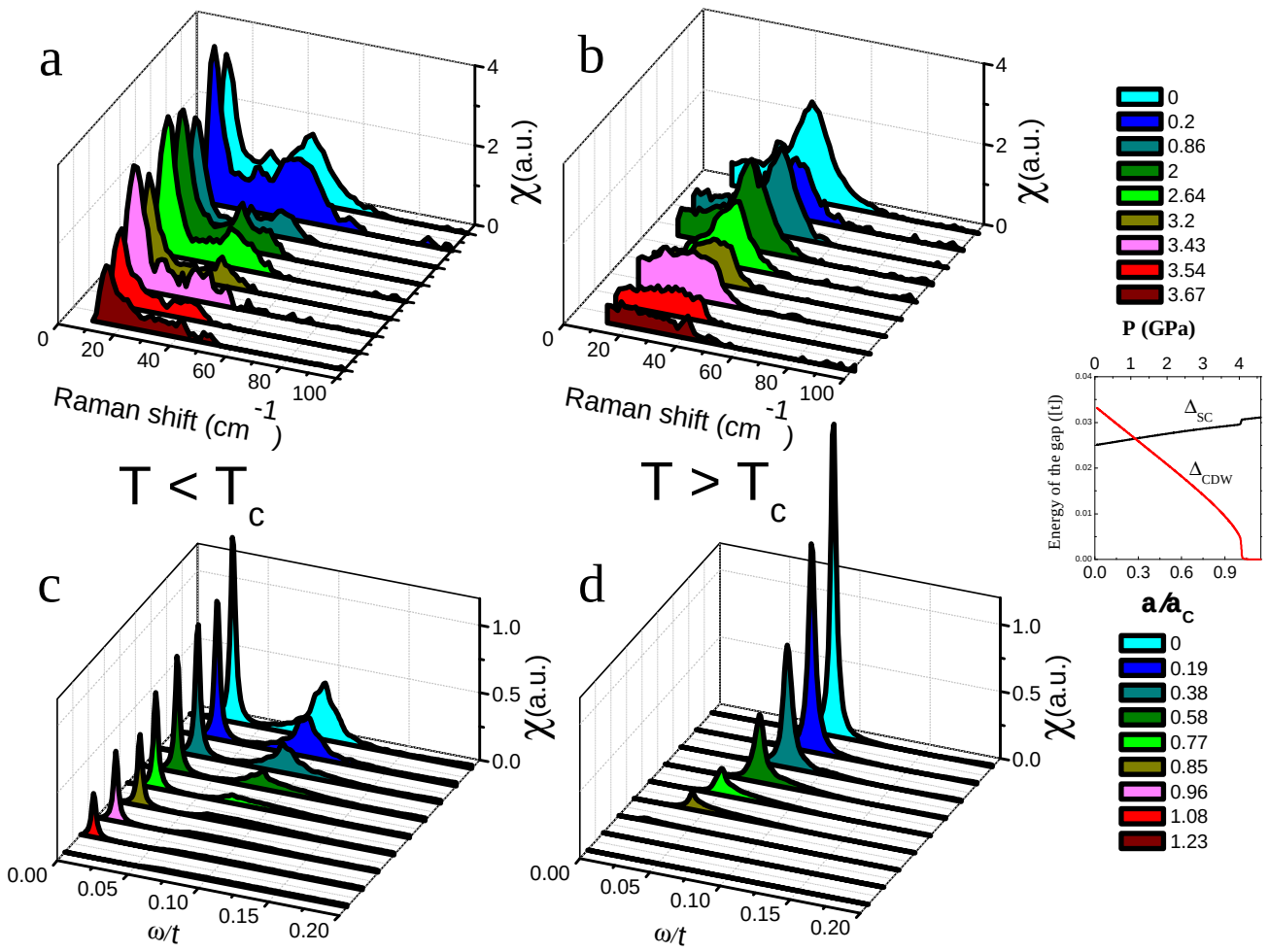

FIG. 3. Pressure dependence of the Raman spectra of 2H-$NbSe_2$ in the coexisting superconducting and charge-density-wave phases and pure charge-density-wave phase, experiments and theory. (a,b) Raman response in the E_{2g} symmetry at 3 K(a) in the CDW+SC state and 8 K(b) in the CDW state for various pressures up to the critical pressure. Spectra are normalized to the E_{2g} phonon and a constant background has been subtracted. (c,d) Theoretical Raman response computed microscopically. Pressure dependence is simulated by suppressing the CDW coupling g_{CDW}/t. α is defined as $(g_{CDW} - g^0_{CDW})/g^0_{CDW}$ where g^0_{CDW} is the coupling at ambient pressure. Inset: calculated CDW and SC gaps versus α (bottom scale) and pressure (top scale). The rapid decrease of the CDW gap suppresses the Raman intensity Z_{eff} of the phonon peak, in agreement with the experiments. However, below T_c the Higgs mode radiance testifies the existence of a CDW order. The Higgs signature disappears when $\Delta_{CDW}(T = 0)$ vanishes, as observed experimentally.

Peierls mechanism[34], making our approach suitable to include the microscopic ingredients specific of 2H-$NbSe_2$.

VII. CONCLUSIONS

In summary, we report the pressure dependence of the A_{1g} and E_{2g} Raman active modes related to the charge-density-wave and superconducting orders in the transition metal dichalcogenide 2H-$NbSe_2$ up to $\sim$ 5GPa. We showed that the soft CDW modes, the so-called amplitudons, and the sub-gap SC modes collapse in the pure SC state above 4 GPa while only the expected Cooper pairs breaking peak at $2\Delta_{SC}$ persists in the E_{2g} symmetry. In the coexisting CDW and SC state, the CDW modes soften, enlarge and loose intensity while the intensity of the SC modes decreases but remains sizable even when the CDW mode is almost invisible. These results reveal that the radiance of the SC modes guarantees that a residual CDW order is present. At all pressure up to 4 GPa and in both A_{1g} and E_{2g} symmetries, we observed a shift to higher energy of the CDW modes and their enlargement upon entering the SC state as well as a transfer of spectral weight from the CDW modes to the SC modes. The pressure trends of the two intertwined CDW and SC modes are well reproduced by our exact calculation of the Raman response within a microscopic model system for the CDW and SC coexisting states. This implies that CDW and SC order parameters must overlap at least in part of the Fermi surface, leading to

the observed coupling between the Higgs modes and the soft CDW modes. Then, our experimental and theoretical findings support the Higgs type assignment of the superconducting modes. Interestingly, from 0 to 4 GPa, the A_{1g} superconducting mode softens by 30% whereas the E_{2g} one is constant. An explanation of this strong symmetry-dependent behavior might requires a calculation within a microscopic model for 2H-$NbSe_2$. Our findings also point out that Raman spectroscopy represents the best suited probe to investigate interplay and competition between charge-density-wave and superconducting coexisting orders, notably when varying the dimensionality, in few-layers systems.

Appendix A: Pure superconducting state at high pressure

In a Raman scattering experiment, superconductivity manifests itself as a Cooper pair breaking peak which consists of a gap opening below $2\Delta_{SC}$ and a gain of spectral weight just above $2\Delta_{SC}$ [22]. It is known that long-range Coulomb screening [40, 41] screens considerably such feature in the fully symmetric A_{1g} channel. Here, as shown Fig. 4, we have probed the pure superconducting (SC) state of 2H-$NbSe_2$ by inducing the collapse of the charge density wave (CDW) under pressure higher than the critical pressure ($P_c \sim 4$ GPa). The broad and weak superconducting peak is measured in the E_{2g} symmetry and as expected for a Cooper pair breaking peak, it is not present in the A_{1g} symmetry (see Fig. 4a).

As pointed out by many recent measurements[46–51], 2H-$NbSe_2$ is an s-wave superconductor with either an anisotropic or multi-gaps. This property affects the shape of the superconducting Raman Cooper pair breaking peak, and was taken into account by defining a anisotropic gap which varies from a small value of Δ_S=0.92 meV and a larger value of Δ_L=1.38 meV. These values are extracted from STM measurements at ambiant pressure [39] and scaled with T_{SC}(P)[26]. We also add an electronic background (red dots): $\beta(\omega) = a\omega/\sqrt{b + c\omega^2}$. It barely affects the shape of the Cooper pair breaking peak but it is necessary to fully reproduced the spectrum. As shown in Fig. 4b, a good fit is obtained by invoking this in-plane anisotropy. We cannot distinguish here between a multi-gaps or anisotropic gap system and we do not exclude k_z dependency in the real compound 2H-$NbSe_2$. Mainly our fit provides evidence for the nature of the superconducting peak above P_c, i.e. a Cooper pair breaking peak, with insight into the energy scales of the superconducting gap.

Appendix B: Spectral weight transfer

Below P_c and upon entering the superconducting state the Higgs mode rises while the CDW mode looses spectral weight. This spectral weight transfer, as illustrated in Fig. 5(a), is observed at every pressure up to the collapse of both modes. This demonstrates a clear coupling between the two modes all throught the P-T phase diagram and further shows the requisite of the charge density wave mode to the visibility of the Higgs mode.

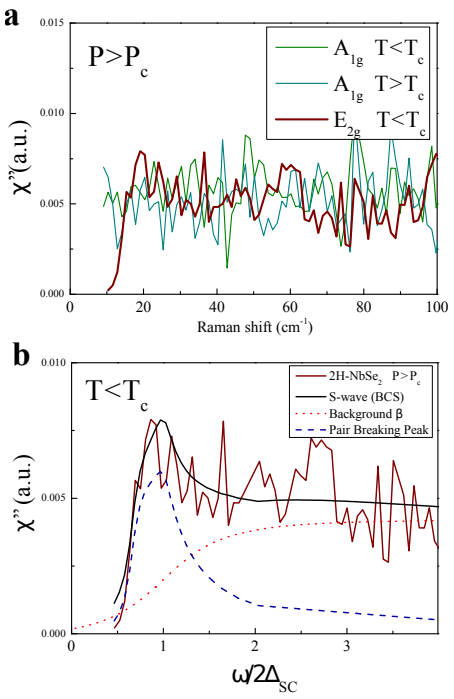

FIG. 4. (a) Superconducting Raman response of 2H-$NbSe_2$ in the pure superconducting phase above P_c in the E_{2g} symmetry below T_{SC} and in the A_{1g} symmetry below and above T_{SC}. (b) Comparison of the superconducting Raman responses of 2H-$NbSe_2$ ($\sim$ 5 GPa) in the pure superconducting phase to the theoretical Raman response of a Cooper pair breaking peak. The Raman shift is normalized to $2\Delta_{SC}$ measured by STM [39],[45]. The black line is the theoretical Raman response of a two-gaps (or anisotropic gap) s-wave superconductor in the BCS regime with an additionnal electronic background β (see text). The value of the gap Δ_{SC} was scaled at high pressure accordingly to the increase of T_{SC} with pressure [26].

The total spectral weight of the two modes above and below T_{SC} as a function of pressure and in the A_{1g} and E_{2g} symmetries is reported Fig. 5(b) and (c). It tends to decrease with increasing pressure in the E_{2g} symmetry whereas there is no clear tendency in the A_{1g} one. The error bars were extracted by integrating the spectral weight of a flat section of the same Raman spectra. Note that the A_{1g} response is extracted from substraction of spectra making the spectral weight calculation generally noisier. As shown in the insets, the spectral weight does not show clear deviation from the behavior versus temperature[6], i.e. a conservation between above and below T_{SC}. But the error bars we obtained while changing the pressure are large and the conservation is respected at only $\pm$20% in the E_{2g} symmetry.

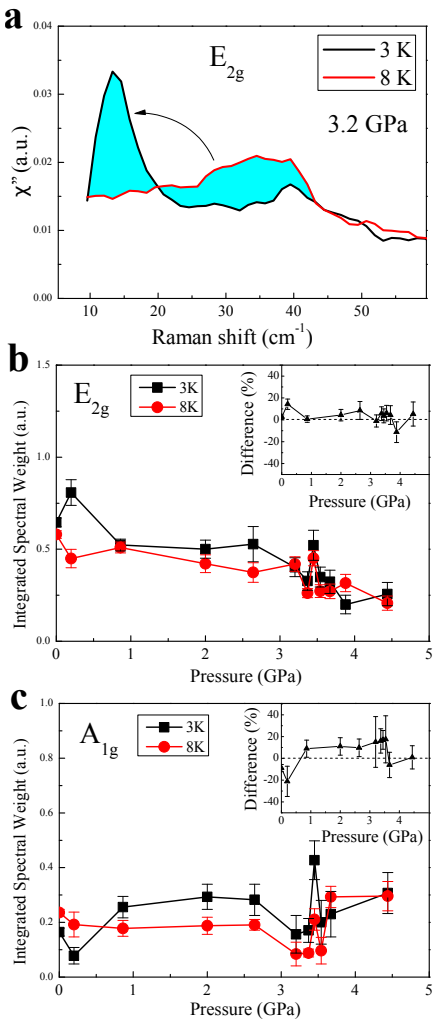

FIG. 5. Spectral weight transfer between the superconducting mode and the charge-density-wave mode. (a) Raman spectra of 2H-$NbSe_2$ at 3.2 GPa above and below T_{SC} in the E_{2g} symmetry. The spectral weight transfer is depicted in blue. (b,c) Total spectral weight of both modes at various pressure below (3 K) and above (8 K) T_{SC} in both E_{2g} and A_{1g} symmetries. Insets: Difference (in %) of spectral weight between these two temperatures as a function of pressure.

Appendix C: Charge density wave modes

Figure 6 presents the pressure dependence of the energy of the Raman active modes associated with the charge-density-wave state, i.e. the soft E_{2g} CDW modes measured at about 40 cm^{-1}, the so-called amplitudon (see Fig. 6(a)), and the single phonon mode at 190 cm^{-1} (see Fig. 6(b)). The E_{2g} amplitudon, as well as the A_{1g} one (not reported), softens towards zero energy with increasing pressure up to the critical pressure (at about 4 GPa) where the CDW collapses, then following the diminishing CDW gap with pressure. It is also shifted to higher energy upon entering the SC phase, due to the coupling with the Higgs fluctuations of the superconducting state. The A_{1g} amplitudon presents qualitatively the same behavior.

On the contrary, the high energy mode which is measured in both the A_{1g} and E_{2g} symmetries, hardens linearly with pressure in the same way the regular phonons do. More precisely, the rate of increase of the normalized energy of the A_{1g}, E^1_{2g} and the CDW-phonon is similar at about 1% per GPa.

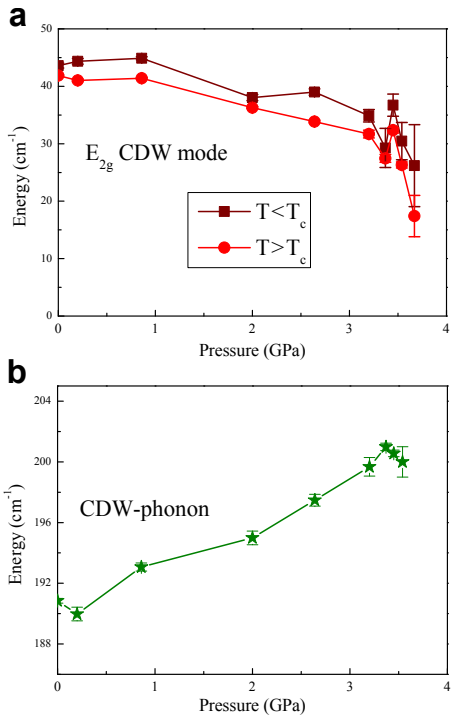

FIG. 6. Evolution of the energy of the CDW modes as a function of pressure. (a) Low energy soft CDW phonon (amplitudon) above and below T_{SC} in the E_{2g} symmetry. (b) Evolution of the energy of the high energy CDW mode ($190 cm^{-1}$) at 8 K.

Appendix D: Theoretical model

The general derivation of the Raman response in the coexisting CDW+SC state has been recently provided in Ref.[4]. Its explicit form depends on the band structure and on the electron-phonon coupling. In order to simplify the derivation we adopt here the same model system used in Ref. [4]. Even thought it does not provide a complete microscopic description of 2H-$NbSe_2$, it contains the main ingredient needed to describe the interplay of CDW and SC in this system, i.e a momentum-dependent CDW, which leaves part of the Fermi surface ungapped below T_{CDW}. This condition makes energetically possible a SC gap opening, and it also allows for a coexisting SC and CDW state in part of the Fermi surface, leading to a coupling between the amplitude fluctuations of the two order parameters. We then start from a single-band

model on the square lattice (lattice spacing $a = 1$) with band dispersion $\xi_{\mathbf{k}} \equiv \epsilon_{\mathbf{k}} - \mu = -2t(\cos k_x + \cos k_y) - \mu$, where $t = 1$ is the hopping and μ is the chemical potential. The CDW instability is driven by the microscopic coupling g_{CDW} of the electrons to a phonon of energy ω_0, $H_I = g_{CDW} \sum_{\mathbf{k}\sigma} \gamma_{\mathbf{k}} c^\dagger_{\mathbf{k}+\mathbf{Q}\sigma} c_{\mathbf{k}\sigma} (b^+_{\mathbf{Q}} + b_{-\mathbf{Q}})$, where the $\gamma_{\mathbf{k}} = |\cos k_x - \cos k_y|$ factor modulates the CDW in the momentum space. Near half filling ($\mu = 0$) the nesting of the Fermi surface at the CDW vector $\mathbf{Q} = (\pi, \pi)$ allows for a CDW instability to occur, with new bands $\xi_\pm = -\mu \mp \sqrt{\epsilon^2_{\mathbf{k}} + \Delta^2_{CDW}\gamma^2_{\mathbf{k}}}$ and a CDW order parameter $\Delta_{CDW} = (4g^2/\omega_0) \sum_{\mathbf{k}\sigma} \langle \gamma_{\mathbf{k}} c^\dagger_{\mathbf{k}\sigma} c_{\mathbf{k}+\mathbf{Q}\sigma} \rangle$. The superconductivity originates from a BCS-like interaction term $H_{SC} = -(U/N) \sum_q \Phi^\dagger_\Delta(\mathbf{q}) \Phi_\Delta(\mathbf{q})$, where $\Phi_\Delta(\mathbf{q}) \equiv \sum_{\mathbf{k}} c_{-\mathbf{k}+\mathbf{q}/2\downarrow} c_{\mathbf{k}+\mathbf{q}/2\uparrow}$ is the pairing operator and N is the number of lattice sites. When treated at mean-field level it leads to the following Green's function $G_0^{-1}(\mathbf{k}, i\omega_n)$, defined on the basis of a generalized 4-components Nambu spinor $\Psi^\dagger_{\mathbf{k}}(i\o_n) \equiv (c^\dagger_{\mathbf{k}\uparrow}(i\omega_n), c^\dagger_{\mathbf{k}+\mathbf{Q}\uparrow}(i\omega_n), c_{-\mathbf{k}\downarrow}(-i\omega_n), c_{-\mathbf{k}-\mathbf{Q}\downarrow}(-i\omega_n))$ that accounts for the CDW band folding:

$$G_0^{-1}(\mathbf{k}, i\omega_n) \equiv i\omega_n - \begin{pmatrix} \hat{h} & -\Delta_{SC}\sigma_0 \\ -\Delta_{SC}\sigma_0 & -\hat{h} \end{pmatrix}, \quad \text{(D1)}$$

where $\omega_n = (2n+1)\pi T$ is the fermionic Matsubara frequency, Δ_{SC} is the superconducting gap, σ_i denotes the Pauli matrices and $\hat{h}$ is a 2×2 matrix:

$$\hat{h} = \begin{pmatrix} \epsilon_{\mathbf{k}} - \mu & -\Delta_{CDW}\gamma_{\mathbf{k}} \\ -\Delta_{CDW}\gamma_{\mathbf{k}} & -\epsilon_{\mathbf{k}} - \mu \end{pmatrix}. \quad \text{(D2)}$$

The eigenvalues of the matrix $\hat{h}$ represent the two CDW bands $\xi_\pm$, while in the superconducting state the full Green's function (D1) has four possible poles, corresponding to the energies $\pm E_\pm(\mathbf{k})$, with $E_\pm = \sqrt{\xi^2_\pm + \Delta^2_{SC}}$.

The Raman response of the previous model has been derived in Ref. [4] and in the temperature range $T_{SC} < T < T_{CDW}$ it reads

$$\chi_{RR}(i\Omega_n) = \chi^0_{RR} - \frac{2g^2_{CDW}\omega_0 \chi^2_{R,CDW}(i\Omega_n)}{F(i\Omega_n) - (i\Omega_n)^2}, \quad \text{(D3)}$$

where $\Omega_n = 2\pi n T$ is the bosonic Matsubara frequency, $\chi^0_{RR} = \langle \rho_R \rho_R \rangle$ is the bare electronic Raman response, $\chi_{R,CDW} = \langle \rho_R \delta\Delta_{CDW} \rangle$ is the response function coupling the electronic Raman density ρ_R to the amplitude fluctuations $\delta\Delta_{CDW}$ of the CDW order parameter. $F(i\Omega_n)$ in Eq. (D3 represents the phonon mode dressed by the CDW amplitude fluctuations $\chi_{CDW} = \langle \delta\Delta_{CDW} \delta\Delta_{CDW} \rangle$, so that $F(i\Omega_n) = \omega_0^2[1 + (2g^2_{CDW}/\omega_0)\chi_{CDW}(i\Omega_n)]$, with ω_0 bare phonon frequency at $\mathbf{Q}_{CDW}$. After analytical continuation to real frequencies the renormalized phonon frequency below T_{CDW} is found from the equation $F'(\Omega_0) = \Omega_0^2$. Thus, near Ω_0 Eq. (D3) assumes the form of Eq. (1), with $\Gamma_{ph} \simeq -F''(\Omega_0)$ and $Z_{eff} \simeq 2g^2_{CDW}\omega_0 \chi'^2_{R,CDW}(\Omega_0)$.

In the superconducting state, the phonon mode is also dressed by the superconducting amplitude fluctuations, so that $F(i\Omega_n)$ reads :

$$F(i\Omega_n) = \omega_0^2 \left[1 + (2g^2_{CDW}/\omega_0)\chi_{CDW}(i\Omega_n) - (2g^2_{CDW}/\omega_0)\chi^2_{SC,CDW}/X_{SC}\right] \quad \text{(D4)}$$

Here $\chi_{SC,CDW} = \langle \delta\Delta_{SC} \delta\Delta_{CDW} \rangle$ is the response function measuring the change in the superconducting amplitude induced by a fluctuation of the CDW gap, and vice versa. As we mentioned in the main text, it provides a direct coupling between the phonon mode and the Higgs mode, identified by the superconducting resonance $X_{SC}(i\Omega_n) = 2/U + \chi_{SC}(i\Omega_n)$, where $\chi_{SC} = \langle \delta\Delta_{SC} \delta\Delta_{SC} \rangle$. More specifically, the Higgs resonance occurs when $X'_{SC}(\omega = 2\Delta_{SC}) = 0$. As a consequence, the equation $F'(\omega) = \omega^2$ which defines the poles of the Raman response (D3), acquires an additional solution at $\omega < 2\Delta_{SC}$, that remains undamped since the quasiparticle continuum only starts at $2\Delta_{SC}$. In addition, as it has been discussed in Ref. [4], since part of the Fermi surface is further gapped by the CDW gap, the Higgs mode in the coexisting state is much less affected by the quasiparticle damping than in pure superconductors. This explains why the Higgs resonance coupled to the phonon mode appears so sharp in 2H-$NbSe_2$.

The above Eq.s (D3) and (D4) are generic to any band structure, and explain the general mechanism of generation of the amplitudon and Higgs mode in the mixed CDW+SC state. To evaluate the pressure dependence of the Raman spectra we computed explicitly their evolution in our toy model. The various susceptibilities listed above are then easily derived using the definitions of the various operators and of the Green's function (D1) above. For the sake of simplicity we will consider the half-filled case, which allows for an easier treatment of the fluctuations in both superconducting and CDW sectors, without loss of generality of the main conclusions (see Appendix B of ref. [4] for further details on the case of general filling). We then obtain for the fermionic susceptibility the general structure:

$$\chi_A = \sum_{\mathbf{k}} \frac{R_A(\mathbf{k})}{E_{\mathbf{k}}((i\Omega_n)^2 - 4E^2_{\mathbf{k}})} \tanh(\beta E_{\mathbf{k}}/2) \quad \text{(D5)}$$

where $\beta = 1/T$, $E_{\mathbf{k}} = \sqrt{\epsilon^2_{\mathbf{k}} + \Delta^2_{CDW}\gamma^2_{\mathbf{k}} + \Delta^2_{SC}}$ and the form factor $R_A(\mathbf{k})$ depends on the susceptibility under

consideration:

$$R_{R,CDW} = 8\Gamma(\mathbf{k})\Delta_{CDW}\gamma_{\mathbf{k}}^2\epsilon_{\mathbf{k}}, \quad \text{(D6)}$$

$$R_{CDW} = R_{SC} = 4\epsilon_{\mathbf{k}}^2, \quad \text{(D7)}$$

$$R_{SC,CDW} = -8\Delta_{SC}\Delta_{CDW}\gamma_{\mathbf{k}}^2 \quad \text{(D8)}$$

In the present model the Raman response is found different from zero only in the A_{1g} channel where $\Gamma(\mathbf{k}) = \cos k_x + \cos k_y \propto \epsilon_{\mathbf{k}}$, leading to a term proportional to $\epsilon_{\mathbf{k}}^2$ in Eq. (D6) that survives under momentum integration. For the same reason, we find that the phonon does not couple to the total charge density, as obtained by setting $\Gamma(\mathbf{k}) = 1$ in Eq. (D6). This also means that the phonon response is not screened by the long-range Coulomb interactions, mediated by density fluctuations. Even though the present model does not capture the microscopic band structure of 2H-$NbSe_2$, we expect that a similar mechanism is at play in this system as well, explaining the lack of Coulomb screening of the A_{1g} CDW phonon observed experimentally. The CDW and superconducting order parameters are computed by solving self-consistently the two equations:

$$\Delta_{CDW} = \Delta_{CDW}\frac{2g^2}{\omega_0 N}\sum_{\mathbf{k}}\frac{\gamma_{\mathbf{k}}^2}{E_{\mathbf{k}}}\tanh(\beta E_{\mathbf{k}}/2) \quad \text{(D9)}$$

$$\Delta_{SC} = \Delta_{SC}\frac{U}{2N}\sum_{\mathbf{k}}\frac{1}{E_{\mathbf{k}}}\tanh(\beta E_{\mathbf{k}}/2) \quad \text{(D10)}$$

$$\text{(D11)}$$

Here we performed the calculations for the following choice of parameters at $P = 0$: $\omega_0 = 0.16t$, $g_0 = 0.14t$, $U_0 = 0.97t$. To simulate the effect of pressure we suppressed progressively the CDW effective coupling g^2/ω_0 (see Eq. (D9 above) up to the value $g = 0.12t$, where CDW order disappears. As a consequence $(g^2 - g_0^2)/g_0^2 \simeq 2(g - g_0)/g_0 = 2\alpha$ with the definition of the $\alpha = (g - g_0)/g_0$ given in the text. Simultaneously, we slightly suppressed the SC coupling down to $U = 0.79t$, in order to keep T_c almost constant as in the experiments.

Notice that in principle in the present model at half-filling the direct coupling between the Higgs mode and the Raman density, $\chi_{R,SC} = \langle\rho_R\delta\Delta_{SC}\rangle$ is not zero. This is a quite peculiar effect of the band structure considered, that is not expected to hold in 2H-$NbSe_2$ where the bands are approximately parabolic. In this situation indeed the Raman density scales as the total density and the direct coupling of the Higgs mode to the e.m. field is vanishingly small, as in ordinary superconductors[4, 9, 13]. For this reason we did not include explicitly this coupling in the above calculations, and we refer the reader to Ref. [4] for a discussion of its role.

AKNOWLEDGMENTS

This work was supported by the Labex SEAM (Grant No. ANR-11-IDEX-0005-02), by the French Agence Nationale de la Recherche (ANR PRINCESS, Grant No. ANR-11-BS04-002), by the Italian MIUR (PRINRIDEIRON-2012X3YFZ2) and by the Graphene Flagship. We thank gratefully Chandra Varma for providing insight and motivation, F. Mauri, M. Calandra, P. Rodière, H. Suderow and I. Paul for fruitful discussions and G. Lemarchand and A. Polian for technical support.

[1] P. Lee, T. Rice, and P. Anderson, Solid State Communications **14**, 703 (1974).
[2] G. Grüner, Rev. Mod. Phys. **60**, 1129 (1988).
[3] M. V. Klein, Phys. Rev. B **25**, 7192 (1982).
[4] T. Cea and L. Benfatto, Phys. Rev. B **90**, 224515 (2014).
[5] J. C. Tsang, J. E. Smith, and M. W. Shafer, Phys. Rev. Lett. **37**, 1407 (1976).
[6] M.-A. Méasson, Y. Gallais, M. Cazayous, B. Clair, P. Rodière, L. Cario, and A. Sacuto, Phys. Rev. B **89**, 060503 (2014).
[7] X. Xi, L. Zhao, Z. Wang, H. Berger, L. Forró, J. Shan, and K. F. Mak, Nature Nanotechnology **10**, 765 (2015).
[8] N. Nagaosa, *Quantum Field Theory in Condensed Matter Physics* (Springer, Berlin; New York, 1999).
[9] T. Cea, C. Castellani, and L. Benfatto, Phys. Rev. B **93**, 180507 (2016).
[10] A. F. Volkov and S. M. Kogan, Zh. Eksp. Teor. Fiz. [Sov. Phys. JETP] **65[38]**, 2038[1018] (1973[1974]).
[11] I. O. Kulik, O. Entin-Wohlman, and R. Orbach, Journal of Low Temperature Physics **43**, 591 (1981).
[12] P. B. Littlewood and C. M. Varma, Phys. Rev. B **26**, 4883 (1982).
[13] T. Cea, C. Castellani, G. Seibold, and L. Benfatto, Phys. Rev. Lett. **115**, 157002 (2015).
[14] C. Varma, Journal of Low Temperature Physics **126**, 901 (2002).
[15] D. Sherman, U. S. Pracht, B. Gorshunov, S. Poran, J. Jesudasan, M. Chand, P. Raychaudhuri, M. Swanson, N. Trivedi, A. Auerbach, M. Scheffler, A. Frydman, and M. Dressel, Nat Phys **11**, 188 (2015).
[16] R. Matsunaga, Y. I. Hamada, K. Makise, Y. Uzawa, H. Terai, Z. Wang, and R. Shimano, Phys. Rev. Lett. **111**, 057002 (2013).
[17] R. Matsunaga, N. Tsuji, H. Fujita, A. Sugioka, K. Makise, Y. Uzawa, H. Terai, Z. Wang, H. Aoki, and R. Shimano, Science **345**, 1145 (2014).
[18] D. Pekker and C. Varma, Annual Review of Condensed Matter Physics **6**, 269 (2015).
[19] B. Cheng, L. Wu, N. J. Laurita, H. Singh, M. Chand, P. Raychaudhuri, and N. P. Armitage, Phys. Rev. B **93**, 180511 (2016).
[20] N. Tsuji, Y. Murakami, and H. Aoki, Phys. Rev. B **94**, 224519 (2016).
[21] P. B. Littlewood and C. M. Varma, Phys. Rev. Lett. **47**, 811 (1981).

[22] R. Sooryakumar and M. V. Klein, Phys. Rev. B **23**, 3213 (1981).

[23] G. Blumberg, A. Mialitsin, B. S. Dennis, M. V. Klein, N. D. Zhigadlo, and J. Karpinski, Phys. Rev. Lett. **99**, 227002 (2007).

[24] T. Böhm, A. F. Kemper, B. Moritz, F. Kretzschmar, B. Muschler, H.-M. Eiter, R. Hackl, T. P. Devereaux, D. J. Scalapino, and H.-H. Wen, Phys. Rev. X **4**, 041046 (2014).

[25] C. Berthier, P. Molinié, and D. Jérome, Solid State Communications **18**, 1393 (1976).

[26] H. Suderow, V. G. Tissen, J. P. Brison, J. L. Martínez, and S. Vieira, Phys. Rev. Lett. **95**, 117006 (2005).

[27] Y. Feng, J. Wang, R. Jaramillo, J. van Wezel, S. Haravifard, G. Srajer, Y. Liu, Z.-A. Xu, P. B. Littlewood, and T. F. Rosenbaum, Proceedings of the National Academy of Sciences **109**, 7224 (2012).

[28] M. Leroux, I. Errea, M. Le Tacon, S.-M. Souliou, G. Garbarino, L. Cario, A. Bosak, F. Mauri, M. Calandra, and P. Rodière, Phys. Rev. B **92**, 140303 (2015).

[29] N. E. Staley, J. Wu, P. Eklund, Y. Liu, L. Li, and Z. Xu, Phys. Rev. B **80**, 184505 (2009).

[30] M. M. Ugeda, A. J. Bradley, Y. Zhang, S. Onishi, Y. Chen, W. Ruan, C. Ojeda-Aristizabal, H. Ryu, M. T. Edmonds, H.-Z. Tsai, A. Riss, S.-K. Mo, D. Lee, A. Zettl, Z. Hussain, Z.-X. Shen, and M. F. Crommie, Nature Physics **12**, 92 (2015).

[31] M. D. Johannes, I. I. Mazin, and C. A. Howells, Phys. Rev. B **73**, 205102 (2006).

[32] M. Calandra, I. I. Mazin, and F. Mauri, Phys. Rev. B **80**, 241108 (2009).

[33] X. Zhu, Y. Cao, J. Zhang, E. W. Plummer, and J. Guo, Proceedings of the National Academy of Sciences **112**, 2367 (2015).

[34] F. Flicker and J. van Wezel, Nature Communications **6**, 7034 EP (2015).

[35] F. Weber, S. Rosenkranz, R. Heid, and A. H. Said, Phys. Rev. B **94**, 140504 (2016).

[36] W. G. Fisher and M. J. Sienko, Inorganic Chemistry **19**, 39 (1980).

[37] J. Buhot, C. Toulouse, Y. Gallais, A. Sacuto, R. de Sousa, D. Wang, L. Bellaiche, M. Bibes, A. Barthélémy, A. Forget, D. Colson, M. Cazayous, and M.-A. Measson, Phys. Rev. Lett. **115**, 267204 (2015).

[38] D. Jérome, C. Berthier, P. Molinié, and J. Rouxel, Le Journal de Physique Colloques **37**, C4 (1976).

[39] I. Guillamón, H. Suderow, S. Vieira, and P. Rodière, Physica C: Superconductivity and its Applications **468**, 537 (2008).

[40] T. P. Devereaux and D. Einzel, Physical Review B **51**, 16336 (1995).

[41] T. P. Devereaux and R. Hackl, Reviews of Modern Physics **79**, 175 (2007).

[42] T. Cea and L. Benfatto, Phys. Rev. B **94**, 064512 (2016).

[43] D. A. Browne and K. Levin, Physical Review B **28**, 4029 (1983).

[44] H. Monien and A. Zawadowski, Phys. Rev. B **41**, 8798 (1990).

[45] I. Guillamón, H. Suderow, S. Vieira, L. Cario, P. Diener, and P. Rodière, Phys. Rev. Lett. **101**, 166407 (2008).

[46] Y. Noat, J. A. Silva-Guillén, T. Cren, V. Cherkez, C. Brun, S. Pons, F. Debontridder, D. Roditchev, W. Sacks, L. Cario, P. Ordejón, A. García, and E. Canadell, Phys. Rev. B **92**, 134510 (2015).

[47] D. J. Rahn, S. Hellmann, M. Kalläne, C. Sohrt, T. K. Kim, L. Kipp, and K. Rossnagel, Phys. Rev. B **85**, 224532 (2012).

[48] J. D. Fletcher, A. Carrington, P. Diener, P. Rodière, J. P. Brison, R. Prozorov, T. Olheiser, and R. W. Giannetta, Phys. Rev. Lett. **98**, 057003 (2007).

[49] Y. Jing, S. Lei, W. Yue, X. Zhi-Li, and W. Hai-Hu, Chinese Physics B **17**, 2229 (2008).

[50] J. Rodrigo and S. Vieira, Physica C: Superconductivity **404**, 306 (2004).

[51] S. V. Borisenko, A. A. Kordyuk, V. B. Zabolotnyy, D. S. Inosov, D. Evtushinsky, B. Büchner, A. N. Yaresko, A. Varykhalov, R. Follath, W. Eberhardt, L. Patthey, and H. Berger, Phys. Rev. Lett. **102**, 166402 (2009).